

Experimental report :

Beamline : BM 32 Experiment number : 32 02 625

2-7 Mars 2005

Extension of the resonant scattering technique to liquid crystalline materials without resonant element

P. Fernandes ¹, P. Barois ¹, E. Grelet ¹, F. Nallet ¹, J. Goodby ², M. Hird ², J-S. Micha ³

¹ Centre de Recherche Paul Pascal (CRPP) - CNRS - Pessac, France

² Department of chemistry, University of Hull, Hull, HU6 7RX, UK

³ European Synchrotron Radiation Facility (ESRF) - Grenoble, France

Abstract

X-Ray resonant scattering experiments have been performed on the historical liquid crystalline compound MHPOBC doped with a chemical probe containing a resonant atom (selenium). We thus determined directly for the first time the microscopic layer structure of the ferroelectric subphases ($\text{SmC}_{\text{FI1}}^*$ and $\text{SmC}_{\text{FI2}}^*$) present in MHPOBC¹. Despite the low fraction of the selenium probe, the resonant signal was strong enough to allow a good determination of the fine structure of the ferroelectric phases. A non resonant Bragg reflection was also found in the $\text{SmC}_{\text{FI1}}^*$ phase in pure MHPOBC, consistent with the 3-layer distorted model, but never detected before. These experiments demonstrate that the resonant scattering technique can be extended to liquid crystalline materials without resonant element and may stimulate new studies.

Keywords: Resonant X-Ray Scattering, Liquid Crystals, Free Standing Films, Mixtures

1. Introduction

Resonant scattering of x-rays has been used since 1998 as a unique and powerful tool to overcome the problem of forbidden Bragg reflections in chiral smectic C liquid crystals [1-4]. It is well known that crystal periodicities associated with uniform helical axes do not produce Bragg reflections in conventional crystallography. The reason is that there is no modulation of the electron density associated with the helical axis symmetry. Resonant scattering occurs when the energy of the x-ray beam matches the absorption edge of an element of the sample. In such condition, the response of the resonant electron is so much amplified that the anisotropy of its local environment is no longer negligible. In other words, the structure factor must be taken as a tensor, whereas it reduces to a scalar in conventional crystallography. As a result, resonant Bragg peaks are observed in place of forbidden reflections and the polarization state of the resonant Bragg peaks is governed by the anisotropy of the tensor structure factor [5, 6].

These properties have been successfully used to study the complex structures of the antiferroelectric smectic C phases and related subphases. The fundamental periodicities of the so-called SmC_α^* and ferroelectric phases $\text{SmC}_{\text{FI1}}^*$ and $\text{SmC}_{\text{FI2}}^*$ have been elucidated [1]. Polarization analysis of the resonant Bragg peaks have shown that some of the structural

¹ In the limit that the probe's presence doesn't change the MHPOBC phase diagram

models (so-called Ising models) had to be ruled out [2, 7] whereas high resolution experiments have allowed a fine determination of the complex structure of the $\text{SmC}_{\text{FI2}}^*$ phase [3], consistent with optical studies [8]. The main features of the various phases are summarized in figure 1.

On a technical point of view, only a limited number of resonant elements can be used to conduct resonant scattering on liquid crystal molecules. The absorption edges of light elements such as carbon or oxygen are too low in energy, whereas heavier elements may not be commonly found in liquid crystals. Practically, good candidates are elements of the third line of the periodic classification heavier than silicon (i.e. phosphorus, sulfur and chlorine) and all elements of the fourth line (i.e. metals, arsenic, selenium and bromine). Phosphorus and arsenic, as a trivalent element, are generally not used in thermotropic liquid crystals, but resonance of phosphorus may be useful for structural studies of biological systems. Metals may be convenient for structural studies of metallomesogens. For all other liquid crystalline materials (i.e. most synthetic liquid crystals designed for applications) four elements only are thus available for resonant scattering studies, namely sulfur, selenium, chlorine and bromine. All of them have been successfully used in resonant scattering studies. Resonance at sulfur and chlorine K-edges occurs at low energy (2.47 and 2.82 keV respectively) hence requiring a specific beamline geometry to minimize x-ray absorption (freely suspended samples under a vacuum or a helium flow [1, 2, 10]). Working at higher energies with selenium (12.66 keV) or bromine (13.47 keV) enables air flight paths and device geometries for electric field studies. Experiments in this range have shown that the resonant signal is strong at selenium K-edge [9] whereas it is very weak with bromine for some reason unclear to us [11].

Most liquid crystals of interest however do not possess one of these four elements, preventing direct characterization of their structure. The aim of this paper is to show that x-ray resonant scattering studies can be carried out anyway in such materials by mixing a small amount of a liquid crystal molecule possessing a resonant element with the material of interest. The foreign molecule acts as a probe, which reflects the microscopic structure of the host molecule.

2 – The materials:

We chose the historical MHPOBC compound as the host liquid crystal. MHPOBC is one of the most extensively studied materials exhibiting the antiferroelectric smectic C phase and the related subphases [12]. The chemical formula and the phase sequence are given on figure 2. Since the MHPOBC molecule does not possess any resonant element, it has never been studied by resonant scattering, which means that the microscopic structure of the subphases has never been characterized.

The selenophene liquid crystal PB237 [13] shown on figure 3 was used as a probe. Its molecular architecture is close to MHPOBC, which certainly favors good mixing. The choice of selenium as the resonant element enables simple diffraction conditions at 12.66 keV, available on most synchrotrons.

As always, the first thing to study with binary mixtures of liquid crystals is the phase diagram. Since the aim of the work is to study the structure of MHPOBC, we are interested in mixtures with a small amount of probe. Three mixtures were prepared with weight fraction of 2, 3.5 and 5%. To ensure mixture homogeneity, after mixing the two products with the correct weight fractions, we dissolved the mixture in dichloromethane that was subsequently evaporated (by controlling both temperature and pressure).

The phase transitions were detected by Differential Scanning Calorimetry on a Perkin-Elmer DSC 7 calorimeter. The results of the calorimetry experiments, presented in figure 4, show that the transition temperatures present a small negative shift growing with increasing percentage of probe but that the number of phases in the mixtures remains unchanged.

The resonant X-ray experiments were also tried with the bromine probe presented in figure 5 but no resonant peaks were discovered. This indicates that the choice of resonant atom and resonant probe are critical aspects of the resonant probe technique.

3 – X-ray experiments:

The resonant x-ray scattering experiments were performed at beamline BM32 of the European Synchrotron Radiation Facility (ESRF) in Grenoble, using a three circle diffractometer. The x-ray beam size was set to 50 μm (vertical) x 300 μm (horizontal) at sample position and the diffracted signal was collected by an NaI scintillator mounted on the two-theta arm. The in-plane (vertical) resolution was then $5.3 \cdot 10^{-4} \text{ \AA}^{-1}$.

The liquid crystal samples were prepared as free standing films drawn to a size of 5mm x 25mm with typical thickness of a micrometer. They were mounted in a two stage oven (10 mK resolution) flushed with helium to reduce diffusion by air.

In this geometry, the alignment of the smectic layers was better than 0.01 degrees as determined by transverse theta scans.

The resonant energy E_0 was first determined by an absorption scan through the PB237 material shown on figure 6. The energy of the beam was then set to $E_0 = 12.653 \text{ keV}$.

With the resonant energy set and the free-standing samples in place, we cooled the sample down to a temperature that corresponded to an interesting phase (based on the bulk DSC experiments) and started the search for the resonant peaks. In figure 7 we present the first result proving that the extension of the Resonant X-ray scattering technique works well (the main objective of this article): the 3/2 order doublets characteristic of the 2 layer superlattice of the SmC_A^* phase. Despite the introduction of a small amount of probe the signal obtained is strong enough to allow good detection and is resolved enough to allow determination of the doublet peaks distance from which the helical pitch, due to chirality, can be calculated.

The resonant signal dependence on the percentage of selenium probe represented in figure 8 encourages the generalization of the resonant probe technique. The intensity ratio that also depends on temperature varies almost linearly with probe percentage meaning that we could strongly reduce the amount of probe, minimizing its influence on the LC to study, and still have a comfortably detectable signal.

Changing phase the 3/2 order doublet disappeared and we observed directly and for the first time in MHPOBC^I the 4/3 and 5/3 order peaks characteristic of the 3 layer superlattice of the SmC_{FI}^* phase (figure 9).

Changing phase again the third order peaks disappeared and we observed directly and for the first time in MHPOBC^I the 5/4, 6/4 and 7/4 order peaks characteristic of the 4 layer superlattice of the SmC_{FI2}^* phase (figure 10).

To prove that the peaks observed are not associated with a modulation of the electronic density the resonance (strong energy dependence) of the peaks must be demonstrated. Figure 11 shows that for the 3/2 order peak a change in energy of only 20 eV resulted in the complete extinction of the signal.

Figure 12 shows that for the 5/4 order peak a change in energy of only 10 eV resulted in the complete extinction of the signal.

Attempting to prove the resonance of the 4/3 order peak in the $\text{SmC}_{\text{FI1}}^*$ phase a surprising result was obtained: the 4/3 order peak is non-resonant. Changing the energy of 20 eV had no effect on the peak's intensity (Figure 13), energy shifts as big as 40 eV caused no change on the observed peak. Figure 13 also shows that the peak was temperature dependent, above and below the $\text{SmC}_{\text{FI1}}^*$ phase the peak disappeared, excluding the X-Ray beam's third order harmonic as the peak's cause.

To rule out any probe induced electronic density modulation the same experiments were performed in pure MHPOBC. Never detected before the 4/3 order peak characteristic of the $\text{SmC}_{\text{FI1}}^*$ phase was observed in pure MHPOBC (Figure 14).

4 – Conclusions:

The method of mixing a resonant probe with a non-resonant chiral Liquid Crystal, in order to determine the structure of the ferroelectric subphases, was successful. . Despite the low fraction of the selenium probe, the resonant signal was strong enough to allow a good determination of the fine structure of the ferroelectric phases.

We determined directly and for the first time the microscopic layer structure of the ferroelectric subphases ($\text{SmC}_{\text{FI1}}^*$ and $\text{SmC}_{\text{FI2}}^*$) present in MHPOBC¹.

A non resonant Bragg reflection was also found in the $\text{SmC}_{\text{FI1}}^*$ phase, consistent with the 3-layer distorted model, but never detected before.

These experiments demonstrate that the resonant scattering technique can be extended to liquid crystalline materials without resonant element and may stimulate new studies.

P. Fernandes thank the Portuguese Foundation for Science and Technology (FCT) for financial support.

References

- [1] Structural Characterization of Various Chiral Smectic-C Phases by Resonant X-Ray Scattering, P. Mach, R. Pindak, A.-M. Levelut, P. Barois, H.T. Nguyen, C.C. Huang and L. Furenlid, Phys. Rev. Lett. **81**, 1015, (1998)
- [2] Structures of chiral smectic-C mesophases revealed by polarization-analyzed resonant x-ray scattering, P. Mach, R. Pindak, A.-M. Levelut, P. Barois, H. T. Nguyen, H. Baltes, M. Hird, K. Toyne, A. Seed, J. W. Goodby, C. C. Huang and L. Furenlid, Phys. Rev. E **60**, 6793, (1999)

- [3] Orientational ordering in the chiral smectic-C*_{FI2} liquid crystal phase determined by resonant polarized x-ray diffraction, A. Cady, J.A. Pitney, R. Pindak, L.S. Matkin, S.J. Watson, H.F. Gleeson, P. Cluzeau, P. Barois, A.-M. Levelut, W. Caliebe, J.W. Goodby, M. Hird and C.C. Huang, Phys. Rev. E **64**, 050702(R), (2001).
- [4] Interlayer structures of the chiral smectic liquid crystal phases revealed by resonant x-ray scattering, L. Hirst, S.J. Watson, H.F. Gleeson, P. Cluzeau, P. Barois, R. Pindak, J. Pitney, A. Cady, P.M. Johnson, C.C. Huang, A.-M. Levelut, G. Srajer, J. Pollmann, W. Caliebe, A. Seed, M.R. Herbert, J.W. Goodby and M. Hird, Phys. Rev. E **65**, 041705, (2002)
- [5] D.H. Templeton and L.K. Templeton, Acta Crystallogr. Sect. A **42**, 478 (1986)
- [6] V.E. Dmitrienko, Acta Crystallogr. Sect. A **39**, 29 (1983)
- [7] Tensorial x-ray structure factor in smectic liquid crystals, B. Pansu and A.-M. Levelut, Phys. Rev. E **60**, 6, (1999)
- [8] T. Matsumoto, A. Fukuda, M. Johno, Y. Motoyama, T.Yui, S. Seomun and M. Yamashita, J. Mater. Chem. **9**, 2051 (1999)
- [9] Resonant x-ray scattering study of the antiferroelectric and ferroelectric phases in liquid crystal devices, L. S. Matkin, S. J. Watson, H. F. Gleeson, R. Pindak, J. Pitney, P. M. Johnson, C. C. Huang, P. Barois, A.-M. Levelut, G. Srajer, J. Pollmann, J. W. Goodby, M. Hird – Physical Review E, 2001, vol. 64, n° 021705
- [10] Resonant x-ray scattering at the Se edge in liquid crystal free-standing films and devices, L. S. Matkin, H. F. Gleeson, P. Mach, C.C. Huang, R. Pindak, G. Srajer, J. Pollmann, J. W. Goodby, M. Hird and A. Seed, Appl. Phys. Lett., **76**, 1863 (2000)
- [11] Although measurable, the resonant signal obtained with bromine was very weak. P. Cluzeau, P. Gisse, V. Ravaine, A.-M. Levelut, P. Barois, C.C. Huang, F. Rieutord and H.T. Nguyen, Ferroelectrics, **244**, 301, (2000).
- [12] A.D.L. Chandani, E. Gorecka, Y. Ouchi, H. Takezoe and A. Fukuda, Jpn. J. Appl. Phys., Part 2 **28**, L1265 (1989)
- [13] J.T. Mills, H.F. Gleeson, M. Hird, P. Styring and J.W. Goodby, J. Mater. Chem. **8**, 2385 (1998)

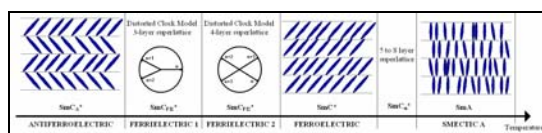
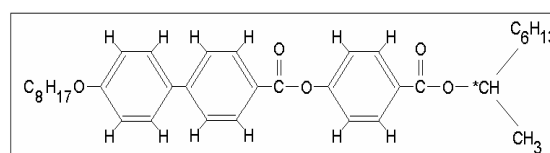
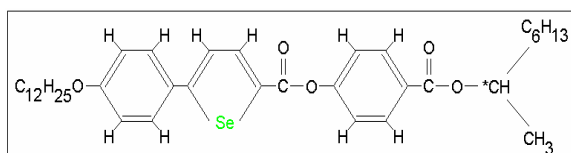


Figure 1 – Schematic representation and general temperature sequence of the various phases observed in chiral antiferroelectric smectic C systems. The superimposed long pitch helical precession has not been represented for clarity.



K 84.0°C SmC_A* 118.4°C SmC_γ* 119.2°C SmC* 120.9°C SmC_α* 122°C SmA 148.0°C Iso

Figure 2 – Structure and phase sequence of MHPOBC.



K 67.7 SmC_A* 97.8 SmC_{FI1}* 99.0 SmC* 109.4 SmA 116.6 Iso

Figure 3 – Structure and phase sequence of PB237 (AS620) – Selenium (K edge=12.66 KeV).

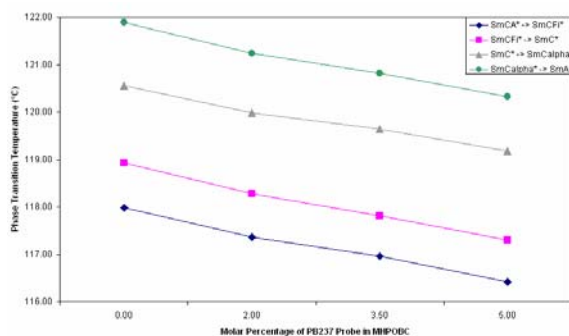


Figure 4 – Temperature shifts of the phase boundaries with increasing fraction of PB237 as detected by DSC scans. Note that the SmC_{FI1}* to SmC_{FI2}* transition is not detected.

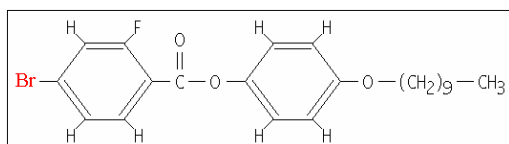


Figure 5 – Bromine probe molecular formula (K edge=13.48 KeV)

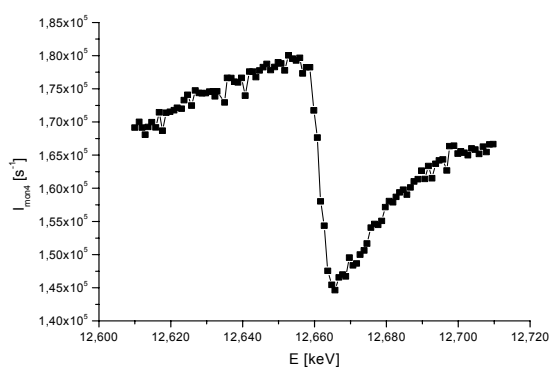


Figure 6 – Absorption scan of the Selenium Probe (PB237 - K edge=12.66 keV).

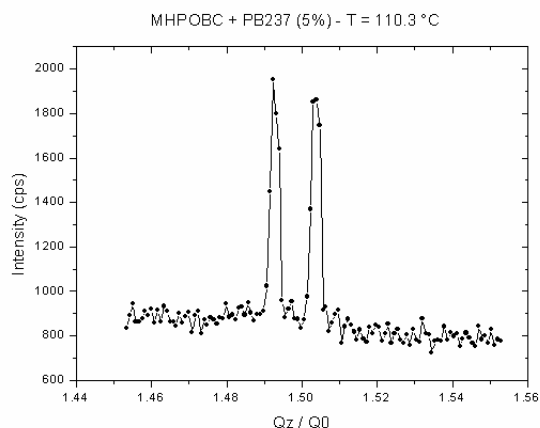


Figure 7 – 3/2 Order Peak in MHPOBC + PB237 (5%), T=110.3°C. Associated Helical Pitch ~91 layers. Layer Thickness~34.5 Å.

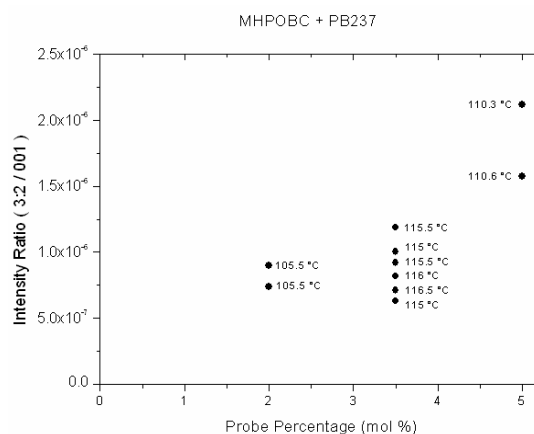


Figure 8 – Intensity ratio dependence of the 3/2:001 peaks with Selenium probe percentage.

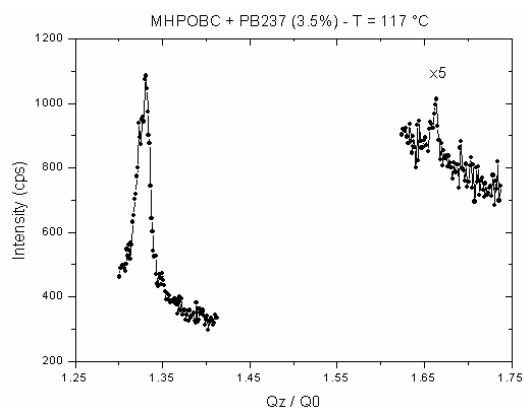


Figure 9 – 4/3 and 5/3 Order Peaks in MHPOBC + PB237 (3.5%), T=117.0°C.

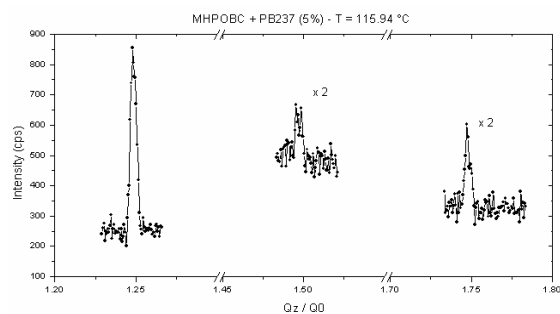


Figure 10 – 5/4, 6/4 and 7/4 Order Peaks in MHPOBC + PB237 (5%), $T=115.9^{\circ}\text{C}$.

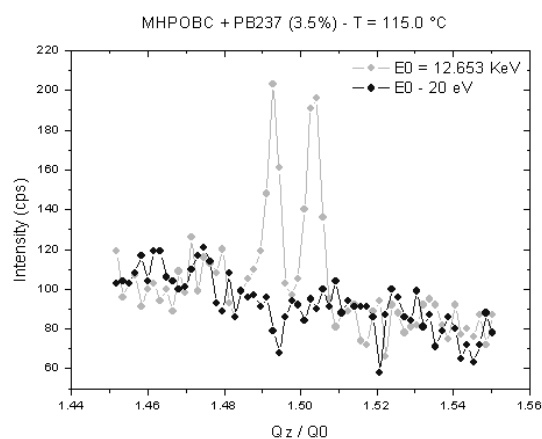


Figure 11 – 3/2 Order Resonant Peak in MHPOBC + PB237 (3.5%), $T=115.0^{\circ}\text{C}$.

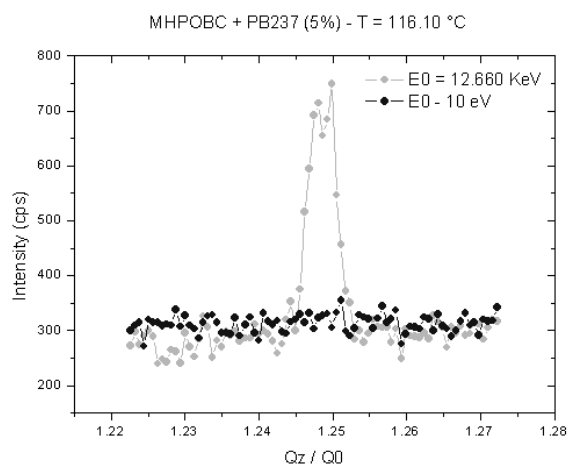


Figure 12 – 5/4 Order Resonant Peak in MHPOBC + PB237 (5%) at $T=116.0^{\circ}\text{C}$ (ratio Intensity 4/3:001=1.06 10-3, ratio FWHM 4/3:001=1.30).

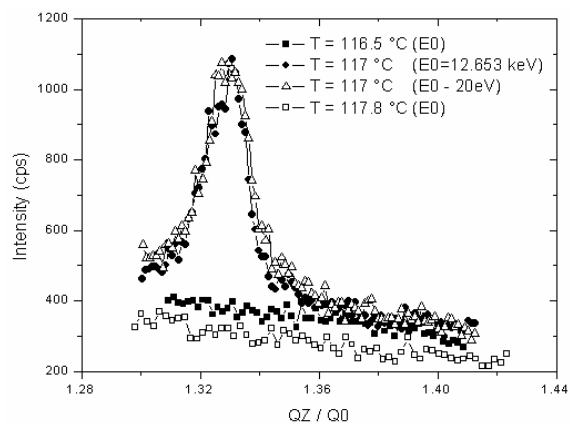


Figure 13 – 4/3 Order Non-Resonant Peak in MHPOBC + PB237 (3.5%) at $T=117.0^{\circ}$ (ratio Intensity 4/3:001=3.28 10-4, ratio FWHM 4/3:001=6.99) and its temperature dependence (disappears at $T=116.5^{\circ}\text{C}$ and $T=117.8^{\circ}\text{C}$).

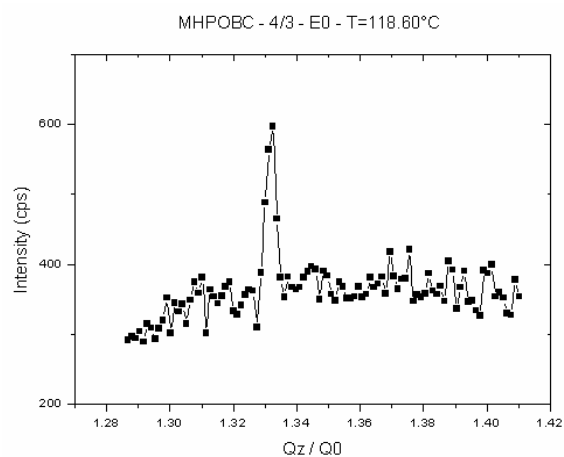


Figure 14 – 4/3 Order Peak in pure MHPOBC at $T=118.60^{\circ}\text{C}$.